

## ARTICLE

# Fabrication and Growth Mechanism of Bamboo-structured Boron Nitride Nanotubes with Thorn-Like Morphology

Jiang Zhang\*, Xi Chen

*Department of Physics, South China University of Technology, Guangzhou 510641, China*

(Dated: Received on March 5, 2014; Accepted on July 21, 2014)

Bamboo-structured boron nitride (BN) nanotubes with thorn-like morphology were synthesized by thermal chemical reaction using amorphous boron powders and NiO nanoparticles as precursors under the flow of  $\text{NH}_3$  at  $1100\text{ }^\circ\text{C}$ . The structural and morphological characteristics of BN nanotubes were investigated by X-ray diffraction and transmission electron microscopy. The results showed that the thorn-like nanostructures attaching to the stems of bamboo-structured BN nanotubes were the hexagonal BN nanoflakes. Based on the diffusion of solid B and vapor  $\text{B}_2\text{O}_2$ , a possible growth mechanism of these novel thorn-like BN nanotubes was primarily proposed.

**Key words:** BN nanotube, Thermal chemical synthesis, X-ray diffraction, Electron microscopy

## I. INTRODUCTION

The discovery of carbon nanotubes [1] motivated the interests in the hexagonal analogs such as boron nitride (BN) and boron carbide ( $\text{BC}_3$ ). Unlike carbon nanotubes, the uniform electronic bandgap (about  $5.5\text{ eV}$ ) of BN nanotubes was predicted to be independent of their diameters, chiralities, and thickness of walls [2]. Hence BN nanotubes can be used as a wide-gap semiconductor. In addition, BN nanotubes have higher thermal and chemical stabilities than carbon nanotubes [3, 4].

In the past decades, many methods, similar to syntheses of carbon nanotubes, such as arc discharge [5, 6], laser ablation [7], and chemical vapor deposition (CVD) with [8, 9] or without [10] metal catalysts, carbon nanotube-confined [11], template-confined method [12], oxide assisted growth method [13], and ball milling method [14, 15] have been applied to synthesize BN nanotubes. Among these methods, the boric CVD technique was considered to be the most effective for the growth of BN nanotubes [16–20]. In this technique, B and metal oxide (such as MgO, FeO, and  $\text{Fe}_2\text{O}_3$ ) were used as the precursors to generate  $\text{B}_2\text{O}_2$  vapors at high temperature ( $>1300\text{ }^\circ\text{C}$ ). Then the vapors reacted with  $\text{NH}_3$  gas to form BN nanotubes in the relative low temperature zone. Generally, BN nanotubes had cylinder or bamboo-like structures. Some BN nanotubes with novel morphology, such as hair-like BN nanotubes [20, 21] and thorn-like BN nanostructures [22, 23] were also fabricated by different methods.

In this work, we reported the fabrication of BN nanotubes by CVD technique using amorphous B powders and NiO nanoparticles as the precursors. The bamboo-structured BN nanotubes with a novel thorn-like morphology were obtained in the  $\text{NH}_3$  atmosphere at  $1100\text{ }^\circ\text{C}$ .

## II. EXPERIMENTS

Amorphous B powder (99.8% purity,  $4\text{ }\mu\text{m}$  in particle size) and NiO nanoparticles (99.9% purity,  $20\text{--}40\text{ nm}$  in particle size) with mole ratio of 5:1 were thoroughly mixed by ball milling for 8 h under the protection of argon atmosphere using a mechanical ball mill system (QMCSB). The mixed powder (100 mg) was placed in a quartz boat and loaded into a quartz tube at the center of the furnace tube. Prior to heating, the furnace tube was vacuumed and flushed several times with high-purity argon to eliminate the residual air in the quartz tube. Under a gas flow of  $\text{NH}_3$  with a rate of  $100\text{ sccm}$ , the furnace was heated to temperature of  $1100\text{ }^\circ\text{C}$  at a rate of  $20\text{ }^\circ\text{C}/\text{min}$  and held at  $1100\text{ }^\circ\text{C}$  for 1 h. After reaction, the furnace was cooled down to ambient temperature under an argon atmosphere. Finally, the white powder of the BN nanotubes was obtained in quartz boat. The product was analyzed by X-ray diffraction with Cu  $\text{K}\alpha$  radiation (XRD, Rigaku D/Max). Samples were also ultrasonically dispersed in ethanol and a droplet of the solution was placed on a copper grid coated with holey carbon film for the transmission electron microscopy (TEM, JEOL JEM-200CX) and the high-resolution transmission electron microscopy (HRTEM, JEOL JEM-2010) observations.

\* Author to whom correspondence should be addressed. E-mail: jonney@scut.edu.cn, FAX: +86-20-87114837

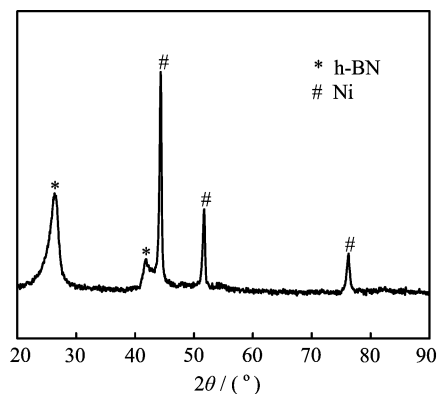


FIG. 1 XRD pattern of the as-prepared product.

### III. RESULTS AND DISCUSSION

XRD was used to investigate the phase structure of the as-prepared product. A typical XRD pattern is shown in Fig.1. All of the peaks can be indexed to hexagonal phase of BN (JCPDS 73-2095) and cubic phase of Ni (JCPDS 04-0850), respectively. No characteristic peaks were observed for any impurities. The XRD results proved the product composition of hexagonal BN (h-BN).

The morphology of the as-prepared product was observed by TEM. Figure 2(a) shows a typical TEM image of BN nanotubes. A number of curved thin bamboo-structured nanotubes with a diameter of 20–40 nm as well as some straight thick nanotubes with a diameter of about 100 nm were observed. The inset of Fig.2(a) is a selected area electron diffraction (SAED) pattern of a cluster of the bamboo-structured nanotubes. The diffraction rings can be indexed to (002) and (100) reflection planes of h-BN, respectively. The as-prepared BN bamboo-structured nanotubes show novel morphology different from those reported in Refs.[20–25]. In the magnified TEM image of the as-prepared BN bamboo-structured nanotubes as shown in Fig.2(b), the thorn-like nanostructures attached to the stem of the tubes were observed. HRTEM image can give the atomic-resolved view of these thorn-like nanostructures. In Fig.2(c), it can be seen that both the stem of the BN nanotube and the curved thorn-like nanostructures are composed of highly crystalline sheets. The distance between the sheets for the thorns is about 0.34 nm, which corresponds to the (002) plane of h-BN. This distance is also the same as that for the stem of the BN nanotube. The results further confirm the as-prepared nanotubes composition of h-BN.

In Fig.3(a), an individual BN nanotube that terminates at a nanoparticle can be observed. The SAED pattern taken from the terminal of the nanotube is shown in Fig.3(b). The diffraction spots and rings can be indexed to the reflection planes of Ni and h-BN, respectively. Obviously, the terminal of the nanotube is

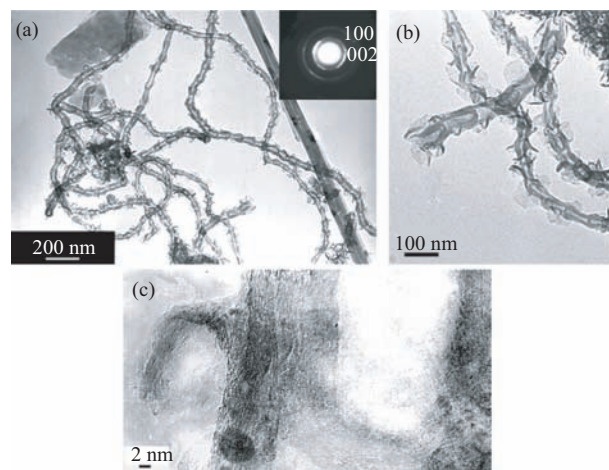


FIG. 2 (a) A typical TEM image of curved bamboo-structured BN nanotubes and straight nanotubes. Inset is corresponding SAED pattern of a cluster of bamboo-structured nanotubes. (b) Magnified TEM of the thorn-like nanostructures. (c) Representative HRTEM image of the thorn-like BN nanotubes.

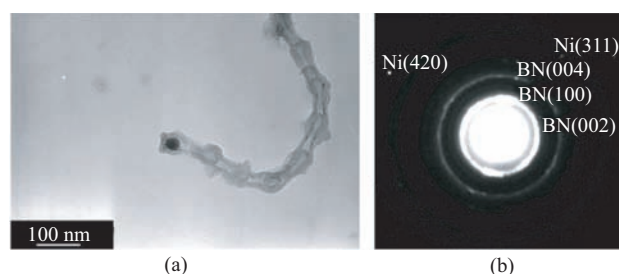


FIG. 3 (a) An individual BN nanotube that terminates at a nanoparticle. (b) Corresponding SAED pattern of the terminal. Diffraction spots and rings can be indexed to Ni (311) and (420) planes and h-BN (002), (100), and (004) planes, respectively.

a Ni nanoparticle enwrapped by h-BN sheets.

In the typical boric CVD technique [16–19], the mole ratio of B to metal oxide was generally 1:1. At high temperature ( $>1300\text{ }^{\circ}\text{C}$ ), it was proposed that most of B could be consumed to generate  $\text{B}_2\text{O}_2$  vapors. Through a vapor transport process, the BN nanotubes grew by a vapor-liquid-solid (VLS) mechanism at low temperature zone. In our experiment, BN nanotubes were *in situ* collected in the quartz boat. No vapor transport process was involved. Obviously the growth mechanism was different from that for the typical boric CVD technique. It should be mentioned that B powders and NiO nanoparticles used as precursors were mixed with B:NiO mole ratio of 5:1. According to the reaction  $2\text{B}(\text{s})+2\text{NiO}(\text{s})\rightarrow\text{B}_2\text{O}_2(\text{g})+2\text{Ni}(\text{l})$ , 80% of B cannot be deoxidized at high temperature ( $1100\text{ }^{\circ}\text{C}$ ). Therefore, both solid B and vapor  $\text{B}_2\text{O}_2$  could supply boron source for the growth of BN nanotubes in our synthesis process. Besides, it is believed that the melting point of

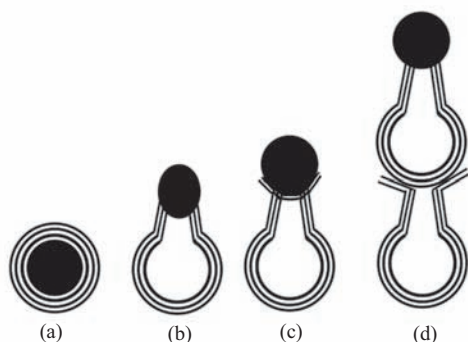


FIG. 4 Schematic diagram of the growth process of the thorn-like BN nanotubes.

the nanoparticles will dramatically decrease due to the nanoscaled size effect [26]. The Ni nanoparticles should be in a quasi-liquid state at 1100 °C although the reaction temperature is lower than the melting point of bulk Ni. Thus the solid-liquid-solid [27] and VLS [28] growth mechanism with tip growth mode are both involved in the formation of these thorn-like BN nanotubes.

Similar morphologies of BN nanostructures, such as hair-like BN nanotubes [20, 21] and thorn-like BN nanostructures [22, 23], have been reported. However, the formation mechanism of these structures was not clear. Based on our experimental results and analysis, a growth mechanism for the formation of these thorn-like BN nanotubes is proposed and illustrated schematically in Fig.4. Firstly, at high temperature, B reacts with NiO to generate Ni nanoparticles and  $B_2O_2$  vapors. Both  $B_2O_2$  and remained B dissolve into the molten Ni nanoparticles. The N atoms decomposed from  $NH_3$  diffuse into the molten Ni nanoparticles and combine with the solute atoms of B to form the BN species. Once the concentrations of species are greater than the saturation threshold, the BN species begin to precipitate in the form of BN shells around the molten Ni nanoparticle (Fig.4(a)). With the growth of the BN layer between the interface of the preformed BN shell and the Ni nanoparticle, the increasing curvature of the newly formed BN shell results in increasing stress energy between the BN shells and the Ni nanoparticle core [29]. When the stress energy overcomes the binding energy of the BN shell, the molten Ni nanoparticle will be expelled and elongate BN shell sequentially, as shown in Fig.4(b). There are two kinds of mechanism proposed to the further growth of nanotubes. In the first point of view, the bulk diffusion of solute atoms, such as C and B, in the liquid metal catalysts dominates the growth of nanotubes [30]. In the second one point of view, the surface diffusion of vapor, such as  $CH_4$ ,  $C_2H_2$  *ect.*, on the surface of the metal catalysts or the nanotubes dominates the growth of nanotubes [31]. It has been reported by Bae *et al.* [27] that the bamboo-structured BN nanotubes were synthesized by thermally treating the mixture powders of B and BN under  $NH_3$

atmospheres in the presence of Fe nanoparticles. They suggested that the bulk diffusion of solid B or BN in Fe nanoparticles dominate the growth process of BN bamboo-structured nanotubes. In our experiment, both the bulk diffusion of solid B and the surface diffusion of vapor  $B_2O_2$  are involved.  $B_2O_2$  vapor can react with  $NH_3$  to form the BN nanoflakes on the monoatomic steps of the Ni surfaces or the edges between the BN layers and the Ni cores, similar to the case presented [31]. On the other hand, the expelled Ni nanoparticle continues to precipitate the supersaturated BN species. Therefore the nanoflakes are extruded out of the stem of BN nanotubes (Fig.4(c)). This process repeats until the B component within the Ni nanoparticle is depleted. The thorn-like bamboo-structured BN nanotubes are sequentially formed (Fig.4(d)). By this token, the bulk diffusion of B dominates the formation of the stem of the BN nanotubes and the surface diffusion of  $B_2O_2$  induces the formation of thorns.

#### IV. CONCLUSION

Novel BN nanotubes with thorn-like morphology have been synthesized simply by thermal chemical reaction of B and NiO under  $NH_3$  atmosphere at 1100 °C. The thorn-like nanoflakes, which are attached to the bamboo-structured BN nanotubes, are composed of crystalline curved h-BN sheets. Both the bulk diffusion of solid B and the surface diffusion of vapor  $B_2O_2$  are involved in the growth of the thorn-like nanotubes. Based on its novel structures, these thorn-like BN nanotubes could be the promising materials in the application areas of hydrogen storage and thermal interface.

#### V. ACKNOWLEDGMENTS

The work was supported by the Fundamental Research Funds for the Central Universities, South China University of Technology (No.2014ZZ0069), the Natural Science Foundation of Guangdong Province (No.6050980), and the National Natural Science Foundation of China (No.10704026).

- [1] S. Iijima, *Nature* **354**, 56 (1991).
- [2] X. Blase, A. Rubio, S. G. Louie, and M. L. Cohen, *Europhys. Lett.* **28**, 335 (1994).
- [3] Y. Chen, J. Zou, S. J. Campbell, and G. Le Caer, *Appl. Phys. Lett.* **84**, 2430 (2004).
- [4] D. Golberg, Y. Bando, K. Kurashima, and T. Sato, *Scr. Mater.* **44**, 1561 (2001).
- [5] N. C. Chopra, R. J. Luyken, K. Cherrey, V. H. Crespi, M. L. Cohen, S. G. Louie, and A. Zettl, *Science* **269**, 966 (1995).

- [6] Y. Saito and M. Maida, *J. Phys. Chem. A* **103**, 1291 (1999).
- [7] D. Golberg, Y. Bando, M. Eremets, K. Takemura, K. Kurashima, and H. Yusa, *Appl. Phys. Lett.* **69**, 2045 (1996).
- [8] O. R. Lourie, C. R. Jones, B. M. Bartlett, P. C. Gibbons, R. S. Rouff, and W. E. Buhro, *Chem. Mater.* **12**, 1808 (2000).
- [9] C. C. Tang, Y. Bando, and T. Sato, *Appl. Phys. A* **75**, 681 (2001).
- [10] R. Ma, Y. Bando, and T. Sato, *Chem. Phys. Lett.* **337**, 61 (2001).
- [11] D. Golberg, Y. Bando, K. Kurashima, and T. Sato, *Chem. Phys. Lett.* **323**, 185 (2000).
- [12] D. Golberg, Y. Bando, W. Han, K. Kurashima, and T. Sato, *Chem. Phys. Lett.* **308**, 337 (1999).
- [13] J. Zhang, C. J. Lu, and Z. Q. Li, *Chin. J. Chem. Phys.* **18**, 113 (2005).
- [14] Y. Chen, M. Conway, J. S. Williams, and J. Zou, *J. Mater. Research* **17**, 1896 (2002).
- [15] D. B. Seo, J. Kim, S. H. Park, Y. U. Jeong, Y. S. Seo, S. H. Lee, and J. Kim, *J. Ind. Eng. Chem.* **19**, 1117 (2013).
- [16] D. Golberg, Y. Bando, Y. Huang, T. Terrao, M. Mitome, C. Tang, and C. Y. Zhi, *ACS Nano* **4**, 2979 (2012).
- [17] C. Y. Zhi, Y. Bando, C. C. Tang, and D. Golberg, *Solid State Commun.* **135**, 67 (2005).
- [18] D. Golberg, Y. Bando, C. C. Tang, and C. Y. Zhi, *Adv. Mater.* **19**, 2413 (2007).
- [19] C. H. Lee, J. S. Wang, V. K. Kayatsha, J. Y. Huang, and Y. K. Yap, *Nanotechnology* **19**, 455605 (2008).
- [20] C. C. Tang, Y. Bando, X. X. Ding, S. R. Qi, and D. Golberg, *J. Am. Chem. Soc.* **124**, 14550 (2002).
- [21] F. L. Deepak, C. P. Vinod, K. Mukhopadhyay, A. Govindaraj, and C. N. R. Rao, *Chem. Phys. Lett.* **353**, 345 (2002).
- [22] W. S. Jang, S. Y. Bae, J. Park, and J. P. Jae, *Solid State Commun.* **133**, 139 (2005).
- [23] X. B. Bi, Y. C. Yin, J. B. Li, Y. J. Chen, J. Li, and Q. Q. Su, *Solid State Sci.* **25**, 39 (2013).
- [24] C. C. Tang, X. X. Ding, X. T. Huang, Z. W. Gan, S. R. Qi, W. Liu, and S. S. Fan, *Chem. Phys. Lett.* **356**, 254 (2002).
- [25] K. F. Huo, Z. Hu, J. J. Fu, H. Xu, X. Z. Wang, and Y. N. Lu, *J. Phys. Chem. B* **107**, 11316 (2003).
- [26] A. N. Goldstein, C. M. Echer, and A. P. Alivisatos, *Science* **256**, 1425 (1992).
- [27] S. Y. Bae, H. W. Seo, J. Park, Y. S. Choi, J. C. Park, and S. Y. Lee, *Chem. Phys. Lett.* **374**, 534 (2003).
- [28] S. Amelinckx, X. B. Zhang, D. Bernaerts, X. F. Zhang, V. Ivanov, and J. B. Nagy, *Science* **265**, 635 (1994).
- [29] X. X. Zhang, Z. Q. Li, G. H. Wen, K. K. Fung, J. L. Chen, and Y. D. Li, *Chem. Phys. Lett.* **333**, 509 (2001).
- [30] Y. T. Lee, J. Park, Y. S. Choi, H. Ryu, and H. J. Lee, *J. Phys. Chem.* **106**, 7614 (2002).
- [31] S. Helveg, C. Lopez-Cartes, J. Scheested, P. L. Hansen, B. S. Clausen, J. R. Rostrup-Nielsen, F. Abild-Pedersen, and J. Norekov, *Nature* **427**, 426 (2004).